



Insights into combustion mechanisms of variable aluminum-based iron oxide/-hydroxide nanothermites



Jakob Hübner^{a,b}, Martin Klaumünzer^{a,*}, Marc Comet^a, Cédric Martin^a, Loïc Vidal^c,
Michael Schäfer^a, Carola Kryschi^b, Denis Spitzer^a

^a *Nanomatériaux pour les Systèmes Sous Sollicitations Extrêmes (NS3E), ISL-CNRS-UNISTRA UMR 3208, French-German Research Institute of Saint-Louis, 5, rue du Général Cassagnou, B.P. 70034, 68301 Saint-Louis, France*

^b *Department of Chemistry and Pharmacy, Institute of Physical Chemistry I and ICMM, Friedrich-Alexander-University Erlangen-Nuremberg, Egerlandstraße 3, 91058 Erlangen, Germany*

^c *Institute of Material Science, University Haute-Alsace, Rue Jean Starcky 15, 68057 Mulhouse, France*

ARTICLE INFO

Article history:

Received 4 January 2017

Revised 8 June 2017

Accepted 13 June 2017

Keywords:

Al-nanoparticles
Iron oxide/-hydroxide nanoscaled matrix
Coprecipitation
Nanothermite
Surface activation
Thermite reactivity

ABSTRACT

Aluminum/iron oxide/-hydroxide nanothermite compounds were prepared and investigated in detail. The fast and facile synthesis was undertaken via a coprecipitation route of iron precursor species (sulfate, chloride) in presence of aluminum nanoparticles with an average diameter of 100 nm, terminated by an amorphous Al_2O_3 passivation layer. The only difference during synthesis is temperature, leading to a non-magnetic (at 20 °C) and magnetic (at 50 °C) nanothermite. HR-TEM and XRPD analysis reveal a predominantly amorphous iron oxide/-hydroxide nanoscaled matrix surrounding the aluminum nanoparticles. Moreover, aluminum nanoparticles and nanoscaled iron oxide/-hydroxide build up a hierarchical $\text{Al}/\text{Al}_2\text{O}_3/\text{Fe}_x\text{O}_y/\text{H}_2\text{O}$ core/shell/shell structure in the case of the magnetic nanothermite. The non-magnetic nanothermite system lacks this significant structure. Finally, as-synthesized systems highly differ in reactivity, which is explained by their individual structural discrepancies. Values of flame propagation velocities and distinct threshold values of sensitivity to electrostatic discharge align with comparable reported aluminum/iron oxide aero- and xerogels in the literature.

© 2017 The Combustion Institute. Published by Elsevier Inc. All rights reserved.

1. Introduction

Exothermic reactions between metallic reducing agents, such as aluminum, and metal oxides were developed and firstly described by the German chemist Johannes Wilhelm Goldschmidt at the end of the nineteenth century [1,2]. These energetic mixtures became famous under the name “thermite” [3]. The large heat release which is often sufficient to heat product phases over their melting points features this type of reaction. For example, the thermite reaction of aluminum and iron(III) oxide can attain temperatures over 3000 °C which is clearly above the melting points of elemental Fe (1538 °C) and Al_2O_3 (2072 °C) [4]. Therefore thermite

reactions found usage in a lot of metallurgical applications. Most common application is the welding of rail tracks. For this purpose, thermites were employed in 1899 for the first time. In 1997 cutting edge research in this field led to the first nanostructured thermites [5]. In subsequent years, a high number of publications demonstrated the outstanding properties of nanothermites: compared to thermites with larger mean particle sizes, nanothermites include a higher sensitivity to electrostatic discharge, small apparent density of loose powder, high propagation rates driven by convection mechanism and high reactive power [6]. This enables nanothermites to be applied as pyrotechnic actuators for projectile guidance [7] or in lead-free ammunition primers [8]. Mixed with high explosive nanoparticles, e.g. RDX, nanothermites can also act as a detonation initiator for secondary explosives without primary explosives, such as the common used but highly toxic lead azide [9]. Current research focus upon aluminum nanopowders as reducing metal for nanothermite composites with typical size distributions from 20 nm to 200 nm [10]. Regarding metal oxides, a huge variety of applicable materials exist. The most commonly used are Fe_2O_3 , MoO_3 , CuO , and Bi_2O_3 [11,12]. It remains to mention that also other substances like Fe_3O_4 , I_2O_5 , AlO_4 , periodates, KMnO_4 , sulfates or persulfates can act as oxidizing agents [6,13–18]. However,

Abbreviations: RDX, 1,3,5-trinitroperhydro-1,3,5-triazine; $\text{Al}/\text{Al}_2\text{O}_3$, passivated aluminum nanoparticle; XRPD, X-ray powder diffraction; TEM, transmission electron microscopy; HR-TEM, high resolution transmission electron microscopy; TEM-EDS, transmission electron microscopy energy dispersive x-ray spectroscopy; TGA, thermogravimetric analysis; DSC, differential scanning calorimetry; PMMA, poly(methyl methacrylate); TNT, 2,4,6-Trinitrotoluol; NdFeB, neodymium rod magnet; $\text{Fe}_x\text{O}_y/\text{H}_2\text{O}$, various iron oxide and hydroxide intermediates; DLVO-theory, named after Derjaguin, Landau, Verwey and Overbeek; MDM, melt dispersion mechanism.

* Corresponding author.

E-mail address: martin.klaumuenzer@isl.eu (M. Klaumünzer).

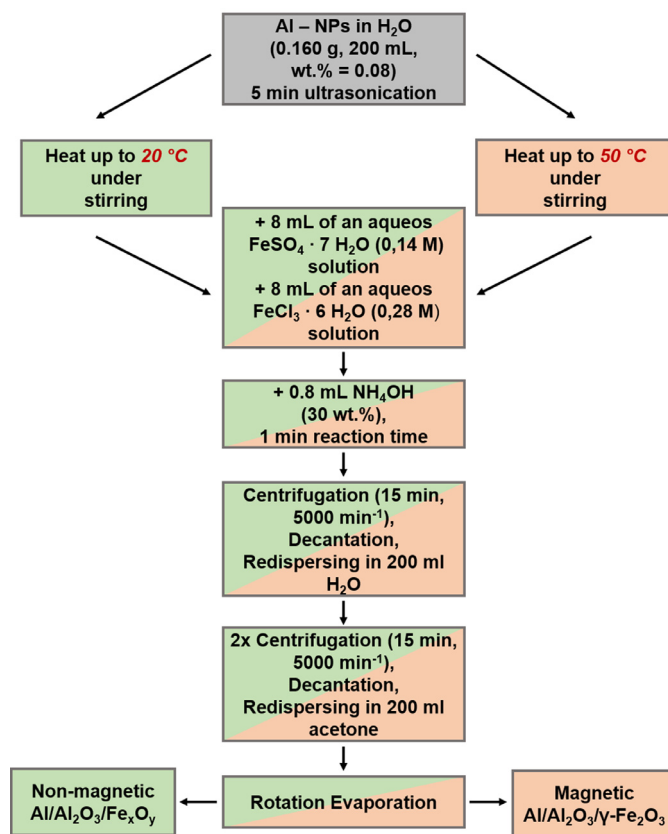
Fe_2O_3 and its intermediates are promising metal oxide/-hydroxide candidates for aluminum nanothermite mixtures because of their strong varying reaction behavior due to diverse synthesis routes. In the literature aluminum/ Fe_2O_3 nanothermite systems are produced by sol-gel synthesis as well as physical mixing or milling processes [19–22]. The strong influence of these different synthesis methods is most noticeable when regarding combustion velocity. Arrested reactive milled aluminum/ Fe_2O_3 nanothermite mixtures offer a combustion velocity of only 0.5 m/s, whereas physical mixed systems combust with 9–80 m/s. In contrast to the latter, results of nanothermite systems mixed by gelation, called xerogels or aerogels, already deflagrate with 320 m/s. Aerogels even reach 895 m/s [11,23]. Moreover, xero- and aerogel aluminum/ Fe_2O_3 nanothermites have a strong difference in sensitivity to electrostatic discharge. The xerogel shows no reaction at a spark energy over 1000 mJ, whereas the aerogel reacts at an energy of 30 mJ [24]. Therefore aluminum/ Fe_2O_3 aerogels are suitable dual use candidates for military or civil applications in primers (e.g. munition, airbags) [9,11]. The convincing virtue of these compounds compared to commonly used lead and mercury containing primers is their non-toxic reaction products. One drawback of xero- and aerogels is given by the elaborate synthesis routes which may take even a couple of days [24,25]. Therefore, the production is expensive and less interesting to the industry. On the other hand, the advantage of Fe_2O_3 as an oxidizing agent in nanothermites is its miscellaneous crystal structure. Especially its ferrimagnetic γ -phase is useful since it shows superparamagnetic behavior when the particle size is decreased below 10 nm [26]. Chemically mixed aluminum/ γ - Fe_2O_3 nanothermite systems (e.g. core-shell structures) would consequently combine advantages of the tunable reaction behavior as well as the applicability of external magnetic fields.

On that score, this paper presents a fast synthesis method for variable non-magnetic and magnetic aluminum/iron oxide/hydroxide nanothermites via coprecipitation of Fe(II) and Fe(III) species, adapted from Massart [27]. In present case, passivated aluminum nanoparticles with an average diameter of 100 nm are synchronously added to the reaction mixture. Resulting nanothermites are characterized in detail using high resolution transmission electron microscopy (HR-TEM), energy-dispersive X-ray spectroscopy (EDS) and high speed analysis of decomposition kinetics, flanked by thermogravimetric (TGA) and differential scanning calorimetry (DSC) studies as well as X-ray powder diffraction (XRPD). Furthermore, building mechanisms of both systems are proposed. Concerning as-prepared materials, the sensitivities to electrostatic discharge are finally compared and discussed.

2. Experimental

2.1. Synthesis

Iron (III) chloride hexahydrate ($\text{FeCl}_3 \cdot \text{H}_2\text{O}$) was purchased from Fluka GmbH (Buchs, Switzerland). Iron (II) sulfate heptahydrate ($\text{FeSO}_4 \cdot 7\text{H}_2\text{O}$), acetone (CHROMASOLV®) and ammonium hydroxide (NH_4OH , 30 wt%) were purchased from Sigma Aldrich (Munich, Germany). Spherical aluminum nanoparticles ($\text{Al}/\text{Al}_2\text{O}_3$ -np) with an average diameter of 100 nm and an amorphous Al_2O_3 passivation layer of 3 nm thickness were obtained from Intrinsiq Materials Ltd. (Farnborough, UK). For a typical synthesis an aqueous $\text{Al}/\text{Al}_2\text{O}_3$ nanoparticle suspension was prepared by adding 160 mg $\text{Al}/\text{Al}_2\text{O}_3$ -nanoparticle to 200 mL deionized H_2O (0.08 wt%) in a 500 mL one neck flask and treating the mixture 5 min with ultrasonication. The resulting suspension was heated up to 20 °C (non-magnetic) or 50 °C (magnetic) under stirring inside an oil-bath. Then, 8 mL of an aqueous $\text{FeSO}_4 \cdot 7\text{H}_2\text{O}$ solution (0.14 M) and 8 mL of an aqueous $\text{FeCl}_3 \cdot 6\text{H}_2\text{O}$ (0.28 M) were added. Afterwards, 0.8 mL NH_4OH were



Scheme 1. Flowchart of the experimental pathway.

added at once. After 1 min of reaction time the mixture was centrifuged (15 min, 5000 min^{-1}), decanted and redispersed in 200 mL deionized H_2O by ultrasonication. This suspension was again centrifuged (15 min, 5000 min^{-1}), decanted and then redispersed in 200 mL acetone by ultrasonication. This procedure was repeated once. Afterwards particles were collected by rotation evaporation. The whole experimental pathway is mapped in Scheme 1.

2.2. Analysis methods

X-ray powder diffraction (XRPD) analysis in Bragg–Brentano geometry was performed on a Bruker AXS Advance D8 (Karlsruhe; Germany) X-ray powder diffractometer using $\text{Cu K}\alpha$ radiation ($\lambda = 1.54 \text{ \AA}$) at an acceleration voltage of 40 kV and 40 mA, operating current. Step size for all scans was set to $0.0148^\circ (2\theta)$. Samples were measured as loose powders on a rotated sample holder. Coherence length L_{hkl} was calculated from the full width at half-maximum (FWHM) of single diffraction peaks by using the well-known Scherrer equation assuming Gaussian shaped peaks that were fitted with OriginPro 9.2 [28].

Transmission electron microscopy (TEM), high resolution transmission electron microscopy (HR-TEM) images and TEM-energy dispersive x-ray spectroscopy (TEM-EDS) scans were recorded with a JEOL ARM2000F (Tokyo, Japan) with a nominal point resolution of 0.8 Å at Scherzer defocus. The microscope was operated at 200 kV acceleration voltage.

Thermogravimetric analysis (TGA) data were collected on a Seiko Instruments Exstar 6000 TG/DTA 6200 (Chiba, Japan) Thermogravimetric/Differential Thermal Analyzer within a measurement range from 30 °C to 1000 °C at a heating rate of 5 °C/min under air. Samples were measured inside alumina crucibles.

Differential scanning calorimetry (DSC) measurements were performed on a TA Instruments DSC Q 1000 (New Castle, USA)

Download English Version:

<https://daneshyari.com/en/article/4764457>

Download Persian Version:

<https://daneshyari.com/article/4764457>

[Daneshyari.com](https://daneshyari.com)